REVIEW

Investigation of cardiomyopathy using cardiac magnetic resonance imaging part 2: Rare phenotypes

Ailbhe C O'Neill, Shaunagh McDermott, Carole A Ridge, David Keane, Jonathan D Dodd

Ailbhe C O'Neill, Shaunagh McDermott, Carole A Ridge, David Keane, Jonathan D Dodd, Department of Radiology, St. Vincent's University Hospital, Elm Park, Dublin 4, Ireland
David Keane, Department of Cardiology, St. Vincent's University Hospital, Elm Park, Dublin 4, Ireland
Author contributions: O'Neill AC, McDermott S and Ridge CA wrote different sections of the article; Dodd JD revised the written article and edited all the images; Keane D edited the article and added clinical information to the figures.
Correspondence to: Dr. Jonathan D Dodd, Consultant Radiologist and Associate Professor, Department of Radiology, St. Vincent's University Hospital, Elm Park, Dublin 4, Ireland. j.dodd@st-vincents.ie
Telephone: +353-87-2987313 Fax: +353-1-2694533
Received: January 29, 2012 Revised: May 15, 2012
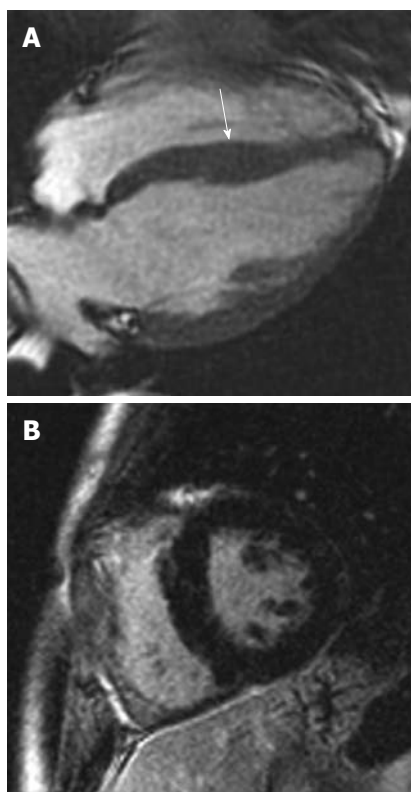Accepted: May 20, 2012
Published online: May 26, 2012

Abstract

Cardiac magnetic resonance imaging (CMRI) has emerged as a useful tertiary imaging tool in the investigation of patients suspected of many different types of cardiomyopathies. CMRI images are now of a sufficiently robust quality to enable high spatial and temporal resolution image acquisition. This has led to CMRI becoming an effective non-invasive imaging tool for many cardiomyopathies. In this two-part review we outline the typical sequences used to image cardiomyopathy and present the imaging spectrum of cardiomyopathy. Part Ⅰ focused on the current classification of cardiomyopathy, the basic CMRI sequences used in evaluating cardiomyopathy and the imaging spectrum of common phenotypes. Part Ⅱ illustrates the imaging spectrum of the more rare phenotypes.

partment of Cardiology, Ibn Rochd University Hospital, Division of Cardiology, Quartier des Hopitaux 20200, Casablanca, Morocco

INTRODUCTION

A cardiomyopathy is described as a myocardial disorder in which the heart muscle is structurally and functionally abnormal, in the absence of coronary artery disease, hypertension, valvular disease or congenital heart disease sufficient to cause the observed myocardial abnormality[1]. It is estimated that cardiomyopathy cause over 26 000 deaths each year in the United States and follows coronary heart disease as the commonest cause of sudden death[2].

Cardiac magnetic resonance imaging (CMRI) has emerged as a useful non-invasive imaging modality capable of producing high-resolution images of the heart in any desired image plane and without ionizing radiation. As a result it has become a primary imaging modality for many cardiomyopathies[3,4]. In this two-part review, we outline the utility of CMRI in the investigation of cardiomyopathies. Part Ⅰ focused on the basic sequences used in characterizing the common cardiomyopathies, reviewed the commonest cardiomyopathy classification systems in use and illustrated the imaging spectrum of the common phenotypes. Part Ⅱ focuses on showing the imaging spectrum of the more rare phenotypes.

RARE CARDIOMYOPATHIES CHARACTERIZED BY HYPERTROPHY

Hypertrophic cardiomyopathy (HCM) is characterized by increased ventricular wall thickness or mass in the ab-
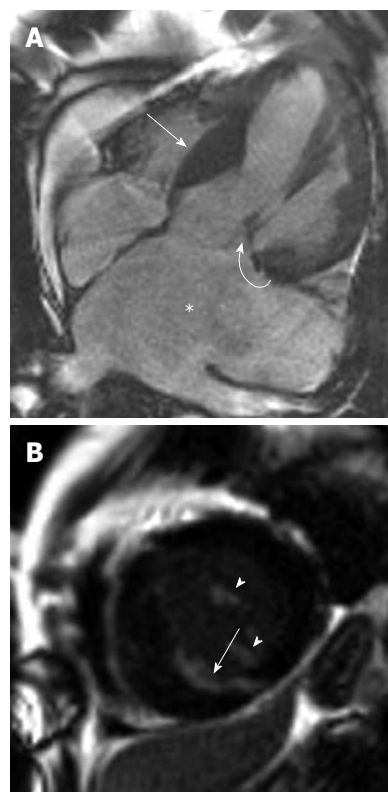
Figure 1 A 19-year-old man with Friedrich's ataxia who presented with sudden onset chest pain. A: Horizontal long-axis SSFP sequence showing circumferential hypertrophy (arrow, 14 mm thickness) of the anterobasal segment of the left ventricular; B: Late-enhanced sequence showing absence of high signal, characteristic of the hypertrophy seen in this disorder.

Figure 2 A 46-year-old man with Noonan's syndrome. A: Horizontal long-axis SSFP sequence showing septal hypertrophy (curved arrow) and a severely dilated left atrium secondary to severe mitral regurgitation (asterisk); B: Late-enhanced short axis sequence showing extensive late gadolinium enhancement (LGE) throughout the antero- and infero-septal myocardial segments (arrow). LGE was also noted in the papillary muscles (arrowheads).

sence of a loading condition such as valvular disease or hypertension. Loading conditions can be volume loading (aortic regurgitation) or pressure loading (aortic stenosis and chronic systemic hypertension).

Friedrich's ataxia

Friedrich's ataxia (FA) is the most common inherited ataxia syndrome. Reduced fraxetin synthesis causes an unstable expansion of a GAA trinucleotide repeat. Clinical features include progressive ataxia, dysarthria, sensory neuropathy, lower limb areflexia, extensor plantar response and weakness secondary to degeneration of dorsal columns and pyramidal tracts[5,6]. Glucose intolerance and various skeletal abnormalities may also be seen. Cardiac involvement in FA is commonly encountered and defined by concentric and symmetrical increased ventricular wall thickness and a normal or small left ventricular (LV) cavity. The systolic function is normal[7].

LV mass on CMRI has been shown to positively correlate with both the genotypic and phenotypic severity of the disease[8]. Increased trinucleotide repeats correlates with increasing LV mass[9]. In particular, septal and posterior wall hypertrophy is more severe in patients with more trinucleotide repeats[8,10]. Larger LV mass is seen with severe and early onset disease. Conversely longer disease duration is often associated with a smaller LV mass. Echocardiography has been the traditional primary imaging tool in FA cardiomyopathy. CMRI offers several additional advantages. It provides a more accurate assessment of the presence, extent and location of myocardial hypertrophy than echocardiography (Figure 1)[8]. It provides these parameters with lower interobserver variation. Perfusion and late contrast enhancement abnormalities indicating myocardial fibrosis can be detected with CMRI early in the pathogenesis of FA cardiomyopathy, earlier than the onset of measurable hypertrophy[11].

Noonan syndrome

Noonan syndrome occurs as a sporadic or autosomal dominant mutation with equal sex predominance[12]. Clinical features include congenital heart defects, bleeding diathesis and mental retardation. Phenotypical features include short stature, hypertelorism, down-slanting eyes, epicanthic folds, low-set posterior ears, micrognathia, a webbed neck and chest deformities[13,14]. Valvular disease is the most common cardiac abnormality. Pulmonary valve stenosis is the most common defect, affecting approximately 50% of patients[15]. Thus, it is important to acquire steady-state free precession sequences of the right ventricular outflow tract (RVOT) and pulmonary valve when evaluating patients suspected of cardiac involvement. Asymmetric septal hypertrophy is seen in 20% of patients with Noonan syndrome (Figure 2)[16,17]. Atrial sep-

tal defects occur in approximately 10%, persistent ductus arteriosus in 3% and ventricular septal defects in 5%[12]. A previous case report has described the CMRI appearances in a patient with Noonan syndrome[17]. In that 27-year-old female the presence of septal hypertrophy was detected with CMRI and shunts were excluded. Late gadolinium enhancement (LGE) manifested as patchy increased signal in the anterior, anteroseptal and lateral walls[17]. Echocardiography remains the primary imaging modality in Noonan's cardiomyopathy. In cases where imaging with echocardiography is equivocal or incongruent with other clinical parameters, CMRI can provide imaging confirmation of hypertrophy.

RARE CARDIOMYOPATHIES CHARACTERIZED BY DILATATION

Dilatation of the cardiac chambers with impaired contraction of the ventricles is characteristic of dilated cardiomyopathies.
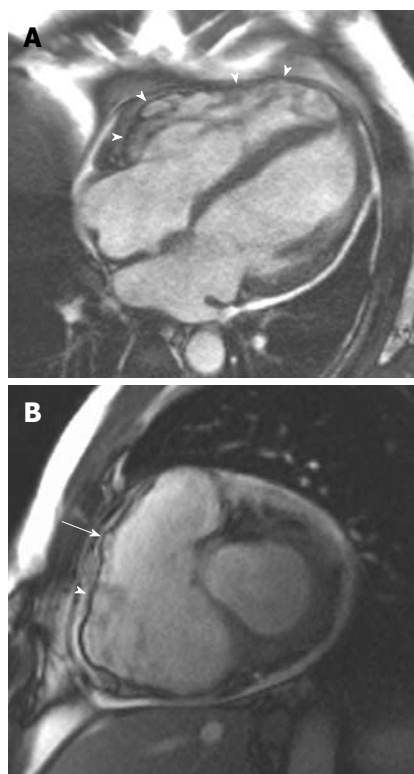
Arrhythmogenic right ventricular dysplasia

Arrhythmogenic right ventricular dysplasia (ARVD) is a rare genetic disorder characterized by progressive loss of myocytes with fibro-fatty replacement of right, and more recently described, LV myocardium. Patients may present with ventricular arrhythmias and left bundle branch block, syncope or sudden cardiac death. It may be responsible for up to 5% of sudden deaths in young athletes[18], although it has a higher prevalence in some countries such as Italy (25% of sudden deaths in young athletes)[19]. Because of the subtlety of the phenotype, consensus criteria were developed based on structural, functional, and electrocardiographic (ECG) manifestations[20]. In these criteria, tissue characterization depicted on CMRI such as fatty infiltration has been removed and an increased emphasis placed on right ventricular wall motion, volume and ejection fraction abnormalities.

CMRI assessment of ARVD is now primarily based on functional and volume abnormalities of the right ventricle[20] although many centers still provide tissue characterization imaging of the right ventricle. Morphological abnormalities include intra-myocardial fat deposits, focal wall thinning (< 2 mm), wall hypertrophy (> 6 mm), moderator band hypertrophy and trabeculation disarray. Functional abnormalities include focal or global RV wall hypokinesis (dilatation, focal or global RV dilatation and in severe cases, focal aneurysms). The site of involvement most commonly occurs in the "triangle of dysplasia" found in the inferior sub-tricuspid area, RV apex and RV infundibulum. The major treatment implication in suspected cases of ARVD is implantable defibrillator placement.

Important CMRI sequences in ARVD

CMRI protocols for ARVD focuses particular attention on the right ventricle and RVOT (Figure 3). A thinner slice thickness and slice gap for this protocol (5-6 mm

Figure 3 A 38-year-old man of Italian origin presented with palpitations and progressive shortness of breath during exercise. A: Horizontal long-axis SSFP shows a heavily trabeculated right ventricle with thickened trabeculae and increased right ventricular (RV) volume. The RV free wall is very thin, with multiple small aneurysms (arrowheads); B: Short-axis SSFP sequence showing further small aneurysms of the RV free wall. Note again the increased RV volume.
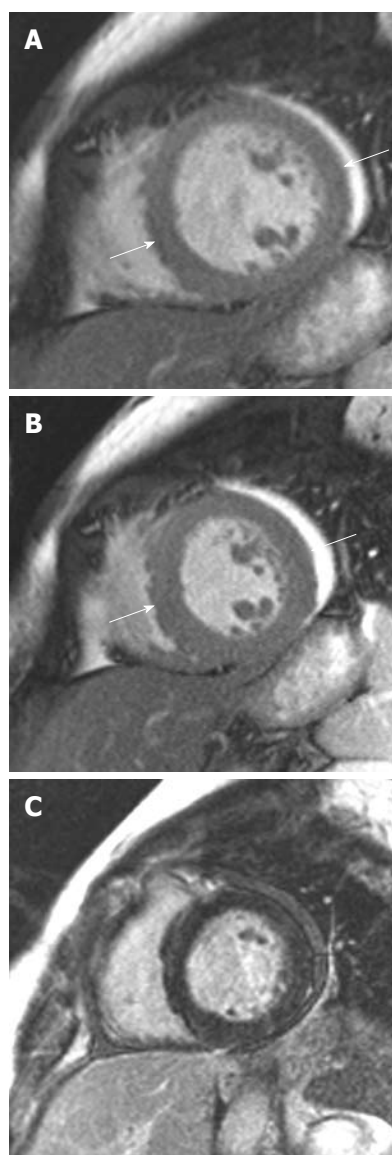
contiguous slices are typical) is recommended. Saturation bands above and below the heart help improve image quality by reducing flow artifacts related to slow-inflowing blood. A small field of view targeted to the right ventricle helps improve the spatial resolution further, at the cost of decreasing signal-to-noise ratio. Myocardial late enhancement has been used to demonstrate scarring of the RV wall[21].

The diagnostic accuracy of CMRI for ARVD carries a high sensitivity but low specificity when compared with traditional Task Force criteria[22]. Modified criteria have been proposed, such that the presence of any minor criterion in a first-degree relative of a proven case of ARVD is regarded as clinical disease expression[20]. When CMRI is assessed using these modified criteria it is frequently abnormal, suggesting a role in depicting initial manifestations of disease[20,23]. It is important to emphasize that the interpretation of CMRI abnormalities should be made in a multidisciplinary approach involving ECG, arrhythmic, morpho-functional, histopathological, and clinical/molecular genetic analysis before making the diagnosis of ARVD[20,24].

Peripartum cardiomyopathy

Peripartum cardiomyopathy (PPCM) is defined as heart failure occurring in the last month of pregnancy or with-

Figure 4 A 34-year-old woman 1 wk post-partum who developed progressive shortness of breath. A: Short-axis SSFP sequence showing dilation of the left ventricle (end-diastolic diameter = 62 mm); B: The systolic phase demonstrating moderate circumferential hypokinesis (left ventricular ejection fraction 45%); C: Late gadolinium enhancement sequence showing an absence of high signal in this case.

in 5 mo of delivery. The etiology of PPCM is multifactorial. Ntusi *et al*[25] and Baruteau *et al*[26,27] divided the etiology of PPCM into inflammatory and non-inflammatory causes. Inflammatory PPCM occurs secondary to viral myocarditis, an abnormal immune response to pregnancy, an abnormal response to hemodynamic stresses of pregnancy, increased myocyte apoptosis and cytokine-mediated myocardial inflammation. Non-inflammatory causes of PPCM include malnutrition, genetic factors, increased prolactin production, abnormal hormone function and increased adrenergic tone.
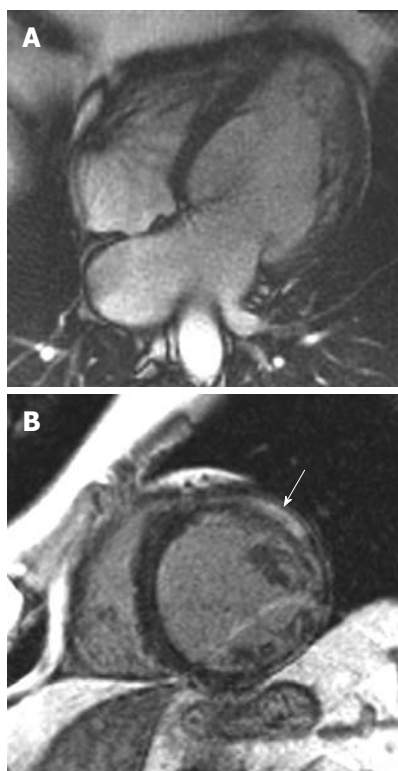
CMRI appearances: It is no surprise with such a multifactorial etiology that the reported CMRI appearances of PPCM are varied. The most common finding is a dilated left ventricle (Figure 4). Reported appearances post administration of gadolinium are more varied. Marmursztejn *et al*[28] described the CMRI appearances of two patients with PPCM. The first patient had a normal post-gadolinium CMRI and at clinical follow-up regained normal cardiac function. The second patient had several areas of myocardial LGE and had persistent LV dysfunction on clinical follow-up. Mouquet *et al*[29] evaluated eight patients with PPCM with CMRI and no LGE was seen in any patient. Kawano *et al*[30] described a case of PPCM with diffuse epicardial and midwall LGE in the left ventricle on CMRI performed at 2 mo with reduction in the LGE on follow-up CMRI at 10 mo. One explanation for the differing reports may lie in the differing inflammatory *vs* non-inflammatory etiologies for PPCM. Those with a predominantly inflammatory etiology demonstrate LGE in a similar fashion to other viral myocarditis as opposed to non-inflammatory etiologies which are not associated with a T2 hypersignal or LGE[27].

Muscular dystrophy

Duchenne and Becker muscular dystrophies are X-linked genetic mutations affecting the dystrophin gene. Dystrophin is totally absent or dysfunctional in Duchenne muscular dystrophy (DMD) and dystrophin is mildly dysfunctional or reduced in expression in Becker muscular dystrophy (BMD). DMD is associated with a more severe disorder and patients die of respiratory failure, rarely surviving past the third decade. In contrast, BMD is a milder form of dystrophy with patients surviving until the sixth decade; cardiomyopathy is the main cause of death[31]. Another important group of dystrophies that may exhibit cardiomyopathy are the limb girdle muscular dystrophies. The subtypes most commonly associated with cardiac involvement include those associated with a defect in the genes coding for the α (LGMD2D), β (LGMD2E), γ (LGMD2C), or θ (LGMD2F) subunits of the dystrophin associated sarcoglycan complex.

CMRI appearances: The subepicardium of the inferolateral wall is initially affected in BMD. This occurs in the third decade of life and increases in extent with age. There is a progressive loss of contractility and decrease in LV systolic dysfunction secondary to ongoing myocardial damage. Cardiac involvement is not commonly seen in patients under the age of 16 with BMD, but increases to 70% by the age of 40 years[32]. Yilmaz *et al*[33] demonstrated that patients with BMD and reduced LV ejection fraction were older, had heavier hearts and regional wall motion abnormalities. In DMD, almost all patients that survive to > 30 years of age demonstrate cardiomyopathy. LGE has been reported involving the inferolateral free wall, the basal inferior and anterolateral region of the left ventricle (Figure 5)[34,35]. The LGE likely occurs because of myocardial damage resulting from mechanical stress on top of a metabolically and structurally abnormal myocardium, although the precise mechanism remains to be elucidated. Whether the inferolateral wall is particularly vulnerable because of

Figure 5 A 46-year-old man with progressive heart failure and Becker's muscular dystrophy. A: Short-axis SSFP sequence showing moderate dilation of the left ventricle; B: Late gadolinium enhancement (LGE) sequence showing extensive transmural LGE throughout the lateral segments (arrow).

regional molecular changes or from exposure to higher mechanical stress is unknown. It is interesting that the LGE pattern is remarkably similar to that of myocarditis, and that enterovirus infection has been shown to produce myocardial damage *via* cleavage of dystrophin[36]. Perhaps this explains the similarity in the LGE pattern between myocarditis and dystrophin-associated cardiomyopathy. Performing CMRI in DMD/BMD is useful because early commencement of standard heart failure therapy can delay the onset and progression of LV systolic dysfunction and possibly even reverse the remodeling process. Furthermore, myocardial fibrosis detected by LGE imaging may be observed in the presence of normal echocardiography[34]. For the limb-girdle muscular dystrophies, several authors have shown LGE in the basal interventricular septum in these cardiomyopathies before the onset of ventricular dilatation and systolic dysfunction[37].

RARE CARDIOMYOPATHIES CHARACTERIZED BY RESTRICTION

Carcinoid heart disease

Carcinoid tumors arise from neuroendocrine tumors and secrete vasoactive substances including 5-hydroxytryptamine, histamine and bradykinin. Clinical symptoms of carcinoid syndrome occur when there is metastatic disease in the liver and symptoms include episodic flushing,

diarrhea and bronchospasm. Carcinoid heart disease occurs in two-thirds of patients with carcinoid syndrome[38]. Most cardiac lesions affect the right side of the heart, which is postulated to be due to paraneoplastic effects of the vasoactive substances secreted into the hepatic veins from liver metastases[39].
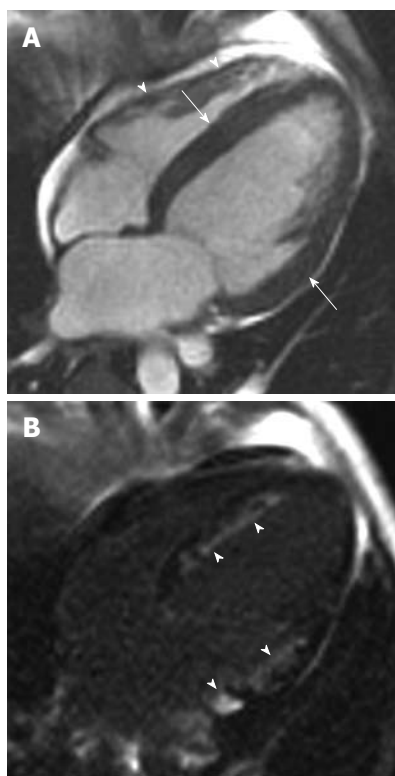
CMRI appearances: Right heart valvular dysfunction is the most common abnormality and the tricuspid valve is most commonly involved[40]. Right atrial and right ventricular enlargement are present in up to 90% of cases of carcinoid heart disease. One study of 252 patients with carcinoid heart disease demonstrated tricuspid valve involvement in 90%, pulmonary valve in 69%, mitral valve in 29% and aortic valve in 27%. Thirteen out of 15 (87%) patients with left-sided cardiac involvement had a patent foramen ovale. Myocardial metastases were seen in 3.8%[41]. Imaging appearances of carcinoid heart disease are of plaque-like deposits causing fibrous endocardial thickening, with retraction and fixation of the valvular cusps and the subvalvular apparatus (chordae and papillary muscles)[42]. Tricuspid valve regurgitation leads to volume overload, which in turn causes right atrial and RV dilatation. In contrast to the tricuspid valve involvement, pulmonary valve involvement typically causes pulmonary stenosis rather than regurgitation[40].

Post contrast delayed CMRI may also demonstrate myocardial fibrosis or scarring as areas of high signal intensity. Several case reports describe similar appearances of cardiac carcinoid on CMRI with right heart chamber dilatation and fixed retraction of the tricuspid valve leaflets. Post contrast images demonstrated enhancement of the tricuspid septal leaflet, most marked at the annulus[43,44].

Hypereosinophilic syndrome

Idiopathic hypereosinophilic syndrome is a syndrome of unknown cause characterized by peripheral eosinophilia and multiorgan dysfunction. Cardiac involvement is common and is characterized by endomyocardial fibrosis and thrombus formation. Three stages are recognized. Stage one is an acute necrotic stage and is clinically silent. There is thrombus formation in stage two. Stage three is characterized by endomyocardial fibrosis and a restrictive cardiomyopathy[45].

CMRI appearances: There are several case reports documenting the appearances of cardiac involvement in hypereosinophilic syndrome on CMRI. A two- or three-layered appearance post contrast is most commonly described, consisting of a normal appearing epicardium, a hyperintense subendocardium indicating eosinophilic infiltration and frequently a linear hypointense layer of thrombus in the endocardium (Figure 6)[46,47]. Histological evaluation has confirmed the presence of endomyocardial eosinophilic infiltration and areas of myocyte necrosis. Debl *et al*[48] have suggested the potential for CMRI to evaluate response to treatment, with a decrease in the
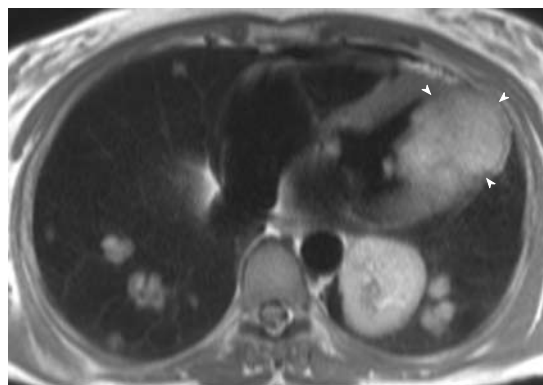
Figure 6 A 38-year-old man presented with progressive shortness of breath. Serum measurements demonstrated hypereosinophilia. A: Horizontal long-axis SSFP sequence showing mild circumferential hypertrophy of the left ventricle (arrows) Note the normal thin right ventricular free wall (arrowheads), a useful differentiating feature from cardiac amyloid; B: Late-enhanced horizontal long-axis sequence showing extensive high signal in the typical subendocardial distribution (arrowheads) of eosinophilic myocardial infiltration. Cardiac amyloid is the principal other cardiomyopathy that mimics this late gadolinium enhancement appearance.

Figure 7 A 56-year-old woman with metastatic sarcoma. Note the diffuse metastatic infiltration of the left ventricle (arrowheads), resulting in restrictive pathophysiology. There are also diffuse pulmonary metastases throughout both lungs.

Figure 8 A 23-year-old man with Rubenstein-Taybi syndrome who presented with increasing shortness of breath. Vertical long-axis view demonstrating increased trabeculations at the apical ventricular level fulfilling cardiac magnetic resonance imaging criteria for left ventricular noncompaction.

extent of late enhancement occurring with successful steroid therapy. Syed *et al*[46] has also described severe hypertrophy of the LV myocardium and partial obliteration of the LV cavity in systole.
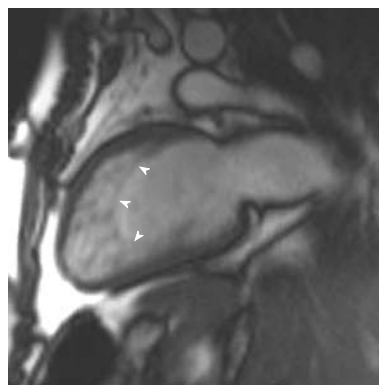
Metastatic disease

Metastatic disease to the heart and pericardium is more common than primary cardiac tumors[49]. Lung carcinoma, lymphoma, breast carcinoma, esophageal carcinoma and melanoma are the most common metastases to the heart[50,51]. Lung carcinoma typically involves the heart through direct invasion, sometimes by transvenous growth through the pulmonary veins. Cardiac metastatic involvement heralds a poor prognosis. "Charcoal heart" is the term peculiar to extensive cardiac melanoma metastases, in which the pathological appearance of the infiltrated myocardium is heavily pigmented.

CMRI appearances: Most cardiac tumors are low signal on T1-weighted sequences and higher signal on T2-weighted sequences (Figure 7)[52]. Typically, metastases enhance post contrast administration. A first pass perfusion sequence may be used to image the enhancement of the tumor with high temporal resolution. If this sequence

is used, its duration should be for longer than the typical 30 s used for ischemic cases, as often the metastases take longer to demonstrate perfusion. Another useful sequence to differentiate metastases from a thrombus mass is the late-enhanced sequence in which the inversion time is set to 600 ms. Metastases enhance whilst a thrombus remains black (no signal).

UNCLASSIFIED CARDIOMYOPATHIES

LV non-compaction (LVNC) and Takotsubo cardiomyopathy (TTC) are unclassified cardiomyopathies.

LV non-compaction

LVNC is a myocardial disorder characterized by prominent, excessive trabeculations and deep intratrabecular recesses (Figure 8). The intratrabecular recesses communicate with the ventricular cavity[53]. It is thought to be due to an arrest in the normal myocardial maturation process. The fetal myocardium has deep recesses between loosely interwoven fibers that communicate with the ventricular cavity. These trabeculations aid oxygen exchange by creat-

ing a larger surface area for diffusion. Once the coronary circulation develops, between the 5th to 8th weeks of life, these trabeculations are no longer needed and the loosely woven fibers undergo compaction[54]. Compaction moves from base to apex, epicardium to endocardium and from the septal to the lateral wall. The severity of LVNC will depend on the timing of the arrest in the myocardial maturation and compaction process. The apex and mid-ventricular lateral segments are more commonly involved in LVNC and this is explained by the compaction process as these areas are last to undergo compaction[55].
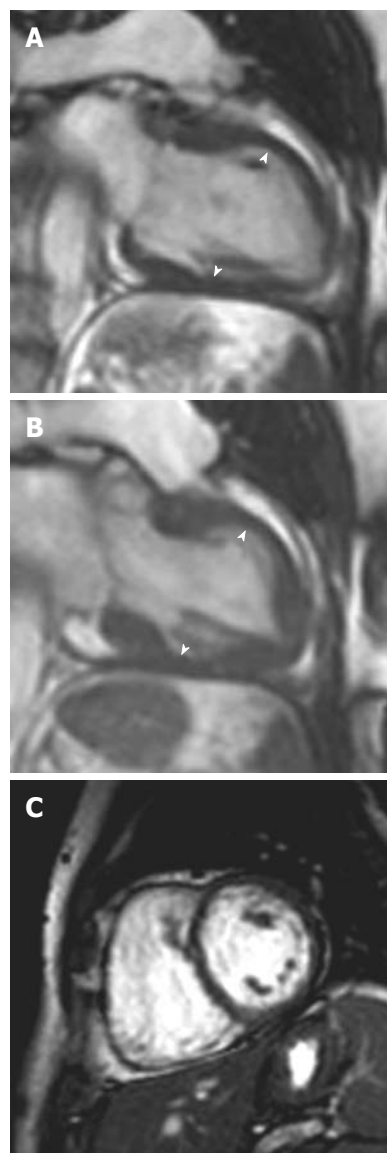
The recesses in LVNC are lined by ventricular endothelium that is in continuity with the ventricular cavity. There is focal ischemic necrosis within the trabeculations and endocardial layer, compensatory hypertrophy of the myocardium, interstitial fibrosis and scarring[56,57]. LVNC was originally described in association with other severe congenital abnormalities and can present as fetal hydrops, neonatal heart failure and ventricular fibrillation[54]. In adults, arrhythmias and thromboembolic events are seen more commonly than in pediatric patients. Cardiac failure is the most common finding in LVNC[53,58]. LVNC may also be seen in association with other congenital cardiac defects. The commonest association is ventricular septal defect, though subaortic obstruction, bicuspid aortic valve, coarctation of the aorta, Ebstein's anomaly, tetralogy of Fallot, pulmonary stenosis and pulmonary atresia are also seen in association with LVNC[59,60].

CMRI appearances: Three basic characteristics of LVNC on CMRI are described; trabeculations of the ventricular wall with deep recesses of the ventricular myocardium, extensive spongiform transformation of the LV myocardium and a dysplastic myocardium that is thinned with excessive trabeculations[61].

The end-diastolic non-compacted to compacted ratio (NC/C) is higher in patients with LVNC. A compaction ratio is calculated by measuring the thickness (in millimeters) of the non-compacted to compacted myocardium. The NC/C parameter separates out pathological non-compaction from less severe forms of non-compaction[62]. This measurement is typically obtained on SSFP sequences with high-resolution thin slices (4-5 mm) on radial slice projections with the fulcrum passing through the center of the left ventricle. The diastolic ratio of > 2.3 on CMRI is diagnostic of LVNC. Further imaging findings on CMRI in LVNC includes trabecular fibrosis, which is seen as delayed enhancement within the trabeculae. Interestingly, delayed enhancement can be seen in non-compacted segments indicating that fibrosis can also affect normal segments[61].

TTC

TTC, also called apical ballooning syndrome or stress cardiomyopathy, is characteristically accompanied by acute chest pain and when associated with ECG changes and elevated troponin, can be erroneously diagnosed as acute coronary syndrome. Clinical criteria for the diagnosis of

Figure 9 A 54-year-old woman with acute onset chest pain and palpitations following a road traffic accident. A, B: Vertical long-axis SSFP sequence in (A) diastole and (B) systole showed akinesis of the left ventricular myocardial segments at the midventricular level; C: Late gadolinium enhancement showing no myocardial enhancement in the involved segments. Subsequent echocardiography 1 mo later showed normal mid-wall contraction.

TTC include transient akinesia or dyskinesia of the LV apical, mid or basal segments beyond the distribution of a single coronary artery, new ECG abnormalities or an elevated troponin, no angiographic evidence of acute plaque rupture or obstructive coronary artery disease, no recent head trauma/intracranial bleeding, no HCM or pheochromocytoma[63,64].

The pathogenesis of TTC is not fully understood. Proposed etiologies include coronary spasm, coronary emboli with spontaneous fibrinolysis, regional myocarditis and abnormalities in the coronary microvascular function. Several studies have demonstrated an association with catecholamine excess. Emotional and physical stressors are often seen in patients with TTC. Plasma levels of neuropeptides and catecholamines in patients with TTC have

been found to be markedly elevated compared to patients with myocardial infarction[65]. One such study described TTC in nine patients, occurring after intravenous infusion of epinephrine or dobutamine[66]. Eitel *et al*[67] evaluated a large group of patients presenting with TTC. In 136 patients with TTC, 121 had significant stressful events 12 h preceding their TTC. Sixty-four patients had emotional stress and 57 had physical stress. Post-menopausal women were more commonly affected, 10% of patients were pre-menopausal, 10% were male and 10% did not recover LV function immediately. Endocardial biopsies in patients with TTC demonstrated changes consistent with catechol-amine excess with contraction bands, increased inflammatory cells and interstitial fibrosis[68].

CMRI appearances: There are several patterns of regional wall motion abnormalities described in TTC[66]. An apical ballooning variant has apical akinesis with sparing of the base and mid-ventricle. A midventricular ballooning variant has midventricular akinesis with sparing of the apex and base (Figure 9). A basal ballooning variant has midventricular and basal akinesis but spares the apex. RV akinesia has also been described in some patients and is associated with lower LV ejection fractions[69]. LGE is seen in patients with myocardial infarctions and myocarditis but not typically in patients with TTC, making CMRI a valuable investigational tool in the work-up of patients suspected of TTC.

REFERENCES

1   **Elliott P**, Andersson B, Arbustini E, Bilinska Z, Cecchi F, Charron P, Dubourg O, Kühl U, Maisch B, McKenna WJ, Monserrat L, Pankuweit S, Rapezzi C, Seferovic P, Tavazzi L, Keren A. Classification of the cardiomyopathies: a position statement from the European Society Of Cardiology Working Group on Myocardial and Pericardial Diseases. *Eur Heart J* 2008; **29**: 270-276

2   **Rosamond W**, Flegal K, Friday G, Furie K, Go A, Greenlund K, Haase N, Ho M, Howard V, Kissela B, Kittner S, Lloyd-Jones D, McDermott M, Meigs J, Moy C, Nichol G, O'Donnell CJ, Roger V, Rumsfeld J, Sorlie P, Steinberger J, Thom T, Wasserthiel-Smoller S, Hong Y. Heart disease and stroke statistics--2007 update: a report from the American Heart Association Statistics Committee and Stroke Statistics Subcommittee. *Circulation* 2007; **115**: e69-171

3   **Bluemke DA**, Achenbach S, Budoff M, Gerber TC, Gersh B, Hillis LD, Hundley WG, Manning WJ, Printz BF, Stuber M, Woodard PK. Noninvasive coronary artery imaging: magnetic resonance angiography and multidetector computed tomography angiography: a scientific statement from the american heart association committee on cardiovascular imaging and intervention of the council on cardiovascular radiology and intervention, and the councils on clinical cardiology and cardiovascular disease in the young. *Circulation* 2008; **118**: 586-606

4   **Pennell DJ**, Sechtem UP, Higgins CB, Manning WJ, Pohost GM, Rademakers FE, van Rossum AC, Shaw LJ, Yucel EK. Clinical indications for cardiovascular magnetic resonance (CMR): Consensus Panel report. *Eur Heart J* 2004; **25**: 1940-1965

5   **Harding AE**. Friedreich's ataxia: a clinical and genetic study of 90 families with an analysis of early diagnostic criteria and intrafamilial clustering of clinical features. *Brain* 1981;

104: 589-620

6   **Dürr A**, Cossee M, Agid Y, Campuzano V, Mignard C, Penet C, Mandel JL, Brice A, Koenig M. Clinical and genetic abnormalities in patients with Friedreich's ataxia. *N Engl J Med* 1996; **335**: 1169-1175

7   **Isnard R**, Kalotka H, Dürr A, Cossée M, Schmitt M, Pousset F, Thomas D, Brice A, Koenig M, Komajda M. Correlation between left ventricular hypertrophy and GAA trinucleotide repeat length in Friedreich's ataxia. *Circulation* 1997; **95**: 2247-2249

8   **Meyer C**, Schmid G, Görlitz S, Ernst M, Wilkens C, Wilhelms I, Kraus PH, Bauer P, Tomiuk J, Przuntek H, Mügge A, Schöls L. Cardiomyopathy in Friedreich's ataxia-assessment by cardiac MRI. *Mov Disord* 2007; **22**: 1615-1622

9   **Rajagopalan B**, Francis JM, Cooke F, Korlipara LV, Blamire AM, Schapira AH, Madan J, Neubauer S, Cooper JM. Analysis of the factors influencing the cardiac phenotype in Friedreich's ataxia. *Mov Disord* 2010; **25**: 846-852

10 **Dutka DP**, Donnelly JE, Nihoyannopoulos P, Oakley CM, Nunez DJ. Marked variation in the cardiomyopathy associated with Friedreich's ataxia. *Heart* 1999; **81**: 141-147

11 **Raman SV**, Phatak K, Hoyle JC, Pennell ML, McCarthy B, Tran T, Prior TW, Olesik JW, Lutton A, Rankin C, Kissel JT, Al-Dahhak R. Impaired myocardial perfusion reserve and fibrosis in Friedreich ataxia: a mitochondrial cardiomyopathy with metabolic syndrome. *Eur Heart J* 2011; **32**: 561-567

12 **Allanson JE**. Noonan syndrome. *J Med Genet* 1987; **24**: 9-13

13 **Zenker M**. Genetic and pathogenetic aspects of Noonan syndrome and related disorders. *Horm Res* 2009; **72** Suppl 2: 57-63

14 **van der Burgt I**. Noonan syndrome. *Orphanet J Rare Dis* 2007; **2**: 4

15 **Shaw AC**, Kalidas K, Crosby AH, Jeffery S, Patton MA. The natural history of Noonan syndrome: a long-term follow-up study. *Arch Dis Child* 2007; **92**: 128-132

16 **Marino B**, Digilio MC, Toscano A, Giannotti A, Dallapiccola B. Congenital heart diseases in children with Noonan syndrome: An expanded cardiac spectrum with high prevalence of atrioventricular canal. *J Pediatr* 1999; **135**: 703-706

17 **Hudsmith LE**, Petersen SE, Francis JM, Robson MD, Watkins H, Neubauer S. Hypertrophic cardiomyopathy in Noonan Syndrome closely mimics familial hypertrophic cardiomyopathy due to sarcomeric mutations. *Int J Cardiovasc Imaging* 2006; **22**: 493-495

18 **Liberthson RR**. Sudden death from cardiac causes in children and young adults. *N Engl J Med* 1996; **334**: 1039-1044

19 **Thiene G**, Nava A, Corrado D, Rossi L, Pennelli N. Right ventricular cardiomyopathy and sudden death in young people. *N Engl J Med* 1988; **318**: 129-133

20 **Marcus FI**, McKenna WJ, Sherrill D, Basso C, Bauce B, Bluemke DA, Calkins H, Corrado D, Cox MG, Daubert JP, Fontaine G, Gear K, Hauer R, Nava A, Picard MH, Protonotarios N, Saffitz JE, Sanborn DM, Steinberg JS, Tandri H, Thiene G, Towbin JA, Tsatsopoulou A, Wichter T, Zareba W. Diagnosis of arrhythmogenic right ventricular cardiomyopathy/dysplasia: proposed modification of the task force criteria. *Circulation* 2010; **121**: 1533-1541

21 **Tandri H**, Saranathan M, Rodriguez ER, Martinez C, Bomma C, Nasir K, Rosen B, Lima JA, Calkins H, Bluemke DA. Noninvasive detection of myocardial fibrosis in arrhythmogenic right ventricular cardiomyopathy using delayed-enhancement magnetic resonance imaging. *J Am Coll Cardiol* 2005; **45**: 98-103

22 **Sen-Chowdhry S**, Prasad SK, Syrris P, Wage R, Ward D, Merrifield R, Smith GC, Firmin DN, Pennell DJ, McKenna WJ. Cardiovascular magnetic resonance in arrhythmogenic right ventricular cardiomyopathy revisited: comparison with task force criteria and genotype. *J Am Coll Cardiol* 2006; **48**: 2132-2140

23 **Sen-Chowdhry S**, Syrris P, Ward D, Asimaki A, Sevdalis E,

McKenna WJ. Clinical and genetic characterization of families with arrhythmogenic right ventricular dysplasia/cardiomyopathy provides novel insights into patterns of disease expression. *Circulation* 2007; **115**: 1710-1720

24   **Jain A**, Tandri H, Calkins H, Bluemke DA. Role of cardiovascular magnetic resonance imaging in arrhythmogenic right ventricular dysplasia. *J Cardiovasc Magn Reson* 2008; **10**: 32

25   **Ntusi NB**, Mayosi BM. Aetiology and risk factors of peripartum cardiomyopathy: a systematic review. *Int J Cardiol* 2009; **131**: 168-179

26   **Baruteau AE**, Leurent G, Schleich JM, Gervais R, Daubert JC, Mabo P. Can peripartum cardiomyopathy be familial? *Int J Cardiol* 2009; **137**: 183-185

27   **Baruteau AE**, Leurent G, Martins RP, Thebault C, Treguer F, Leclercq C, Daubert JC, Mabo P. Peripartum cardiomyopathy in the era of cardiac magnetic resonance imaging: first results and perspectives. *Int J Cardiol* 2010; **144**: 143-145

28   **Marmursztejn J**, Vignaux O, Goffinet F, Cabanes L, Duboc D. Delayed-enhanced cardiac magnetic resonance imaging features in peripartum cardiomyopathy. *Int J Cardiol* 2009; **137**: e63-e64

29   **Mouquet F**, Lions C, de Groote P, Bouabdallaoui N, Willoteaux S, Dagorn J, Deruelle P, Lamblin N, Bauters C, Beregi JP. Characterisation of peripartum cardiomyopathy by cardiac magnetic resonance imaging. *Eur Radiol* 2008; **18**: 2765-2769

30   **Kawano H**, Tsuneto A, Koide Y, Tasaki H, Sueyoshi E, Sakamoto I, Hayashi T. Magnetic resonance imaging in a patient with peripartum cardiomyopathy. *Intern Med* 2008; **47**: 97-102

31   **Emery AE**. The muscular dystrophies. *Lancet* 2002; **359**: 687-695

32   **Nigro G**, Comi LI, Politano L, Limongelli FM, Nigro V, De Rimini ML, Giugliano MA, Petretta VR, Passamano L, Restucci B. Evaluation of the cardiomyopathy in Becker muscular dystrophy. *Muscle Nerve* 1995; **18**: 283-291

33   **Yilmaz A**, Gdynia HJ, Baccouche H, Mahrholdt H, Meinhardt G, Basso C, Thiene G, Sperfeld AD, Ludolph AC, Sechtem U. Cardiac involvement in patients with Becker muscular dystrophy: new diagnostic and pathophysiological insights by a CMR approach. *J Cardiovasc Magn Reson* 2008; **10**: 50

34   **Silva MC**, Meira ZM, Gurgel Giannetti J, da Silva MM, Campos AF, Barbosa Mde M, Starling Filho GM, Ferreira Rde A, Zatz M, Rochitte CE. Myocardial delayed enhancement by magnetic resonance imaging in patients with muscular dystrophy. *J Am Coll Cardiol* 2007; **49**: 1874-1879

35   **Pereira SR**, Silva AS, Bormann EP, Kuppinger O. Association between a new 3q; 5q chromosomal translocation and dystrophy of human retinal pigment epithelium. *Genet Mol Res* 2007; **6**: 1085-1090

36   **Verhaert D**, Richards K, Rafael-Fortney JA, Raman SV. Cardiac involvement in patients with muscular dystrophies: magnetic resonance imaging phenotype and genotypic considerations. *Circ Cardiovasc Imaging* 2011; **4**: 67-76

37   **Raman SV**, Sparks EA, Baker PM, McCarthy B, Wooley CF. Mid-myocardial fibrosis by cardiac magnetic resonance in patients with lamin A/C cardiomyopathy: possible substrate for diastolic dysfunction. *J Cardiovasc Magn Reson* 2007; **9**: 907-913

38   **Kulke MH**, Mayer RJ. Carcinoid tumors. *N Engl J Med* 1999; **340**: 858-868

39   **Møller JE**, Connolly HM, Rubin J, Seward JB, Modesto K, Pellikka PA. Factors associated with progression of carcinoid heart disease. *N Engl J Med* 2003; **348**: 1005-1015

40   **Sandmann H**, Pakkal M, Steeds R. Cardiovascular magnetic resonance imaging in the assessment of carcinoid heart disease. *Clin Radiol* 2009; **64**: 761-766

41   **Bhattacharyya S**, Toumpanakis C, Burke M, Taylor AM, Caplin ME, Davar J. Features of carcinoid heart disease identi-

fied by 2- and 3-dimensional echocardiography and cardiac MRI. *Circ Cardiovasc Imaging* 2010; **3**: 103-111

42   **Mollet NR**, Dymarkowski S, Bogaert J. MRI and CT revealing carcinoid heart disease. *Eur Radiol* 2003; **13** Suppl 4: L14-L18

43   **Martos R**, Ridge C, Quinn M, Dodd J. Cardiac carcinoid: tricuspid delayed hyperenhancement on cardiac 64-slice multidetector CT and magnetic resonance imaging. *Ir J Med Sci* 2010; **179**: 447-449

44   **Mollet NR**, Dymarkowski S, Bogaert J. MRI and CT revealing carcinoid heart disease. *Eur Radiol* 2003; **13** Suppl 6: L14-L18

45   **Weller PF**, Bubley GJ. The idiopathic hypereosinophilic syndrome. *Blood* 1994; **83**: 2759-2779

46   **Syed IS**, Martinez MW, Feng DL, Glockner JF. Cardiac magnetic resonance imaging of eosinophilic endomyocardial disease. *Int J Cardiol* 2008; **126**: e50-e52

47   **Salanitri GC**. Endomyocardial fibrosis and intracardiac thrombus occurring in idiopathic hypereosinophilic syndrome. *AJR Am J Roentgenol* 2005; **184**: 1432-1433

48   **Debl K**, Djavidani B, Buchner S, Poschenrieder F, Heinicke N, Feuerbach S, Riegger G, Luchner A. Time course of eosinophilic myocarditis visualized by CMR. *J Cardiovasc Magn Reson* 2008; **10**: 21

49   **Lam KY**, Dickens P, Chan AC. Tumors of the heart. A 20-year experience with a review of 12,485 consecutive autopsies. *Arch Pathol Lab Med* 1993; **117**: 1027-1031

50   **Mukai K**, Shinkai T, Tominaga K, Shimosato Y. The incidence of secondary tumors of the heart and pericardium: a 10-year study. *Jpn J Clin Oncol* 1988; **18**: 195-201

51   **Klatt EC**, Heitz DR. Cardiac metastases. *Cancer* 1990; **65**: 1456-1459

52   **Fujita N**, Caputo GR, Higgins CB. Diagnosis and characterization of intracardiac masses by magnetic resonance imaging. *Am J Card Imaging* 1994; **8**: 69-80

53   **Oechslin EN**, Attenhofer Jost CH, Rojas JR, Kaufmann PA, Jenni R. Long-term follow-up of 34 adults with isolated left ventricular noncompaction: a distinct cardiomyopathy with poor prognosis. *J Am Coll Cardiol* 2000; **36**: 493-500

54   **Sen-Chowdhry S**, McKenna WJ. Left ventricular noncompaction and cardiomyopathy: cause, contributor, or epiphenomenon? *Curr Opin Cardiol* 2008; **23**: 171-175

55   **Petersen SE**, Selvanayagam JB, Wiesmann F, Robson MD, Francis JM, Anderson RH, Watkins H, Neubauer S. Left ventricular non-compaction: insights from cardiovascular magnetic resonance imaging. *J Am Coll Cardiol* 2005; **46**: 101-105

56   **Burke A**, Mont E, Kutys R, Virmani R. Left ventricular noncompaction: a pathological study of 14 cases. *Hum Pathol* 2005; **36**: 403-411

57   **Jenni R**, Oechslin E, Schneider J, Attenhofer Jost C, Kaufmann PA. Echocardiographic and pathoanatomical characteristics of isolated left ventricular non-compaction: a step towards classification as a distinct cardiomyopathy. *Heart* 2001; **86**: 666-671

58   **Pignatelli RH**, McMahon CJ, Dreyer WJ, Denfield SW, Price J, Belmont JW, Craigen WJ, Wu J, El Said H, Bezold LI, Clunie S, Fernbach S, Bowles NE, Towbin JA. Clinical characterization of left ventricular noncompaction in children: a relatively common form of cardiomyopathy. *Circulation* 2003; **108**: 2672-2678

59   **Lilje C**, Rázek V, Joyce JJ, Rau T, Finckh BF, Weiss F, Habermann CR, Rice JC, Weil J. Complications of non-compaction of the left ventricular myocardium in a paediatric population: a prospective study. *Eur Heart J* 2006; **27**: 1855-1860

60   **Bagur RH**, Lederlin M, Montaudon M, Latrabe V, Corneloup O, Iriart X, Laurent F. Images in cardiovascular medicine. Ebstein anomaly associated with left ventricular noncompaction. *Circulation* 2008; **118**: e662-e664

61   **Dursun M**, Agayev A, Nisli K, Ertugrul T, Onur I, Oflaz H, Yekeler E. MR imaging features of ventricular noncompac-

tion: emphasis on distribution and pattern of fibrosis. *Eur J Radiol* 2010; **74**: 147-151

62   **Cerqueira MD**, Weissman NJ, Dilsizian V, Jacobs AK, Kaul S, Laskey WK, Pennell DJ, Rumberger JA, Ryan T, Verani MS. Standardized myocardial segmentation and nomenclature for tomographic imaging of the heart: a statement for healthcare professionals from the Cardiac Imaging Committee of the Council on Clinical Cardiology of the American Heart Association. *Circulation* 2002; **105**: 539-542

63   **Dote K**, Sato H, Tateishi H, Uchida T, Ishihara M. [Myocardial stunning due to simultaneous multivessel coronary spasms: a review of 5 cases]. *J Cardiol* 1991; **21**: 203-214

64   **Eitel I**, Lücke C, Grothoff M, Sareban M, Schuler G, Thiele H, Gutberlet M. Inflammation in takotsubo cardiomyopathy: insights from cardiovascular magnetic resonance imaging. *Eur Radiol* 2010; **20**: 422-431

65   **Wittstein IS**, Thiemann DR, Lima JA, Baughman KL, Schulman SP, Gerstenblith G, Wu KC, Rade JJ, Bivalacqua TJ, Champion HC. Neurohumoral features of myocardial stun-

ning due to sudden emotional stress. *N Engl J Med* 2005; **352**: 539-548

66   **Abraham J**, Mudd JO, Kapur NK, Klein K, Champion HC, Wittstein IS. Stress cardiomyopathy after intravenous administration of catecholamines and beta-receptor agonists. *J Am Coll Cardiol* 2009; **53**: 1320-1325

67   **Eitel I**, Behrendt F, Schindler K, Kivelitz D, Gutberlet M, Schuler G, Thiele H. Differential diagnosis of suspected apical ballooning syndrome using contrast-enhanced magnetic resonance imaging. *Eur Heart J* 2008; **29**: 2651-2659

68   **Nef HM**, Möllmann H, Kostin S, Troidl C, Voss S, Weber M, Dill T, Rolf A, Brandt R, Hamm CW, Elsässer A. Tako-Tsubo cardiomyopathy: intraindividual structural analysis in the acute phase and after functional recovery. *Eur Heart J* 2007; **28**: 2456-2464

69   **Sharkey SW**, Windenburg DC, Lesser JR, Maron MS, Hauser RG, Lesser JN, Haas TS, Hodges JS, Maron BJ. Natural history and expansive clinical profile of stress (tako-tsubo) cardiomyopathy. *J Am Coll Cardiol* 2010; **55**: 333-341